High-throughput Systems for Behavioral Analysis in Huntington‘s Disease Models

TJC 26.07.2016

Katrin Frauenknecht

Huntington‘s Disease (HD)

- Autosomal dominant neurodegenerative disorder
- Prevalence: 5-10 per 100,000 (western countries)
- Clinical: involuntary movements, cachexia, psychiatric symptoms, dementia
- Mean age of onset: 40y (2-85y) / Mean duration of illlness 17y (2-45y)

- selective loss of GABAergic medium spiny striatal neurons, as well as glutamatergic cortical neurons that project to the striatum

- Gene: Huntingtin (HTT) 4p16.3, 185 kb, 67 exons
- Expanded CAG repeat in the N-terminus of the HTT gene (exon 1)

Animal models of HD – Strain differences

Model	Construct design		Behavioral phenotypes		Neuropathology	
	Promoter and construct	PolyQ length	Onset	Severity	Specificity	Severity
Fragment transgenic models						
R6/2	Human *HTT* promoter, exon 1	144 (variable)	Early	+++	Widespread	+++
N171-82Q	Murine prion promoter, amino acids 1–171	82	Early	+++	Widespread	+++
GFAP-HD	Human GFAP promoter, amino acids 1–208	160	Adult	++	Not assessed	Not assessed
RosaHD	Floxed-STOP *Rosa* locus, exon 1	103	Promoter-dependent		Promoter-dependent	
Full-length human genomic transgenic models						
YAC128	Human *HTT* locus	128	Adult	++	Region-specific	++
BACHD	Human *HTT* locus with exon 1 floxed	97	Adult	++	Region-specific	++
Knock-in models						
Hdh^{Q111}	Human exon 1	111	Late adult	+	Region-specific	+
CAG140	Human/murine exon 1 hybrid	140	Late adult	+	Region-specific	+
Hdh$^{(CAG)150}$	Murine exon 1	150	Late adult	+	Region-specific	+
zQ175	Human/murine exon 1 hybrid	175	Early	++	Region-specific	++

Lee et al. FEBS J. 2013 Sep;280(18):4382-94.

Animal models of HD

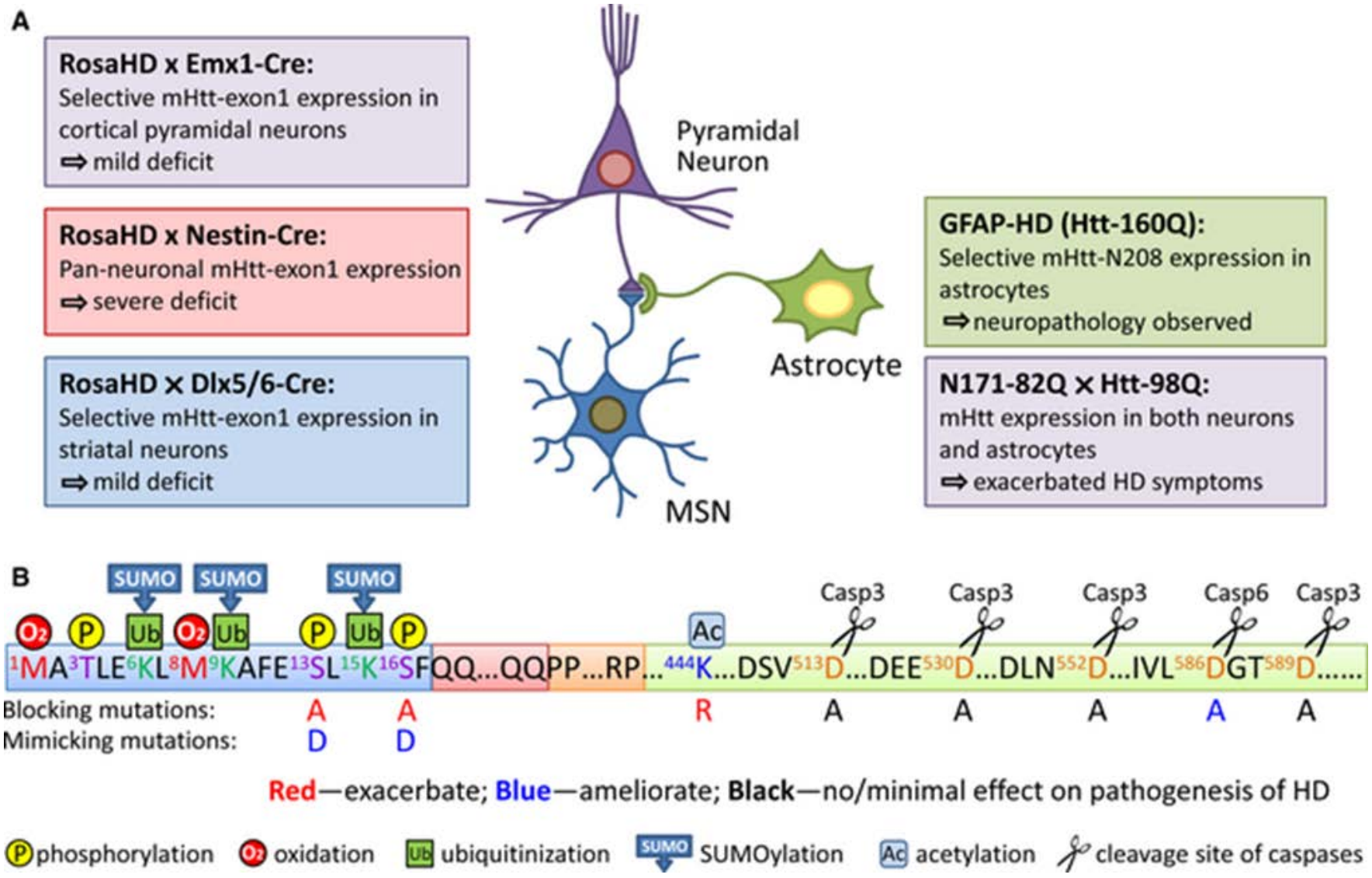

Cre/LoxP conditional mouse models and cell type-specific promoter-driven mHtt models

Lee et al. FEBS J. 2013 Sep;280(18):4382-94.

European Journal of Pharmacology 753 (2015) 127–134

Contents lists available at ScienceDirect

European Journal of Pharmacology

journal homepage: www.elsevier.com/locate/ejphar

Reprint of: Highthroughtput analysis of behavior for drug discovery ☆

Vadim Alexandrov [1], Dani Brunner [*,1], Taleen Hanania, Emer Leahy

PsychoGenics Inc., Tarrytown, New York, USA

Combine behavioral neurobiology insight integrated with advances in robotics and computer vision and the power of bioinformatics to process and analyze massive temporal and vectorial datasets using probabilistic causal interference algorithms

„High-throughput - High content – Unbiased“

Behavioral high-throughput system: IntelliCage

IntelliCage unit (New Behavior AG)

Behavioral high-throughput system: SmartCube

- Predicts the potential utility of CNS active compounds by comparing their behavioral signature to known neuropsychiatric drug signatures
- Uses robotics, computer vision, proprietary algorithms and bioinformatics to
  - Capture and analyze >2000 behavioral features per session (locomotion, trajectory complexity, body posture and shape, simple behaviors and behavioral sequences)
  - Create drug signatures (therapeutic utility, potential side effects, additive/synergistic effects)
- Capacity tom test 10,000 compounds at multiple doses per year

Behavioral high-throughput system: SmartCube

Figure 1

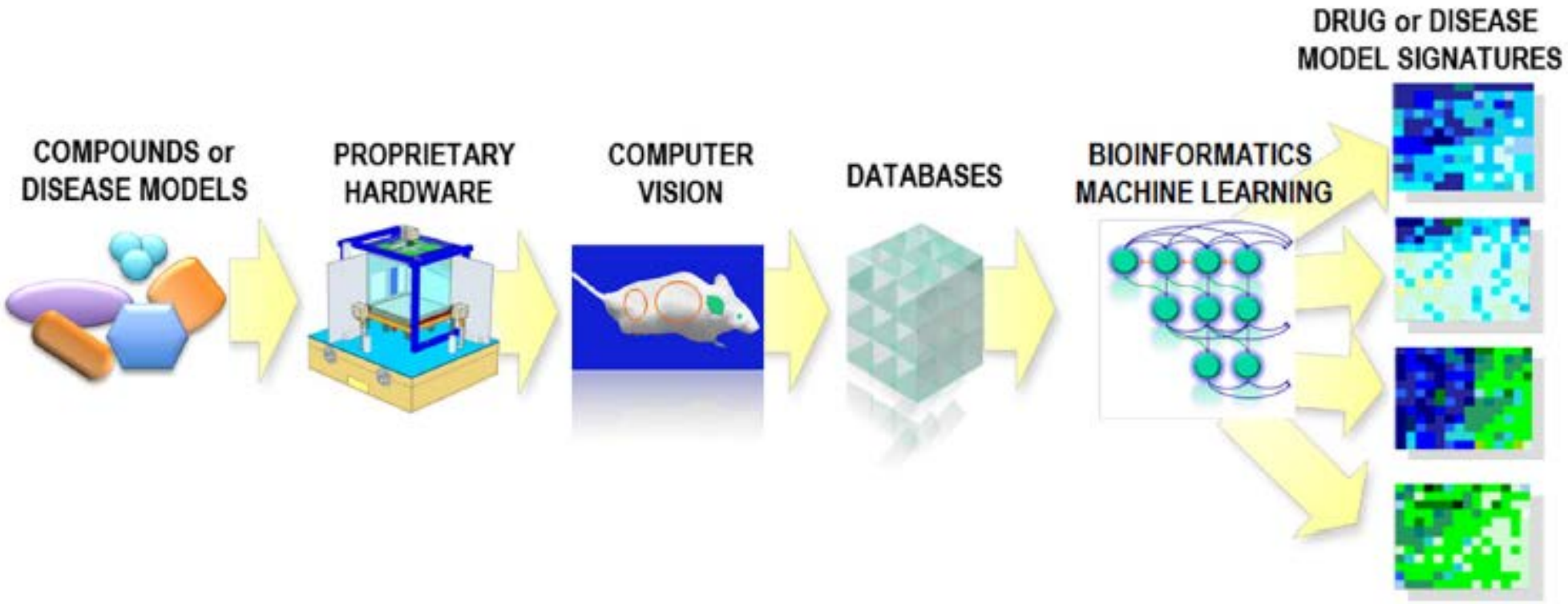

Behavioral high-throughput system: SmartCube

Figure 2

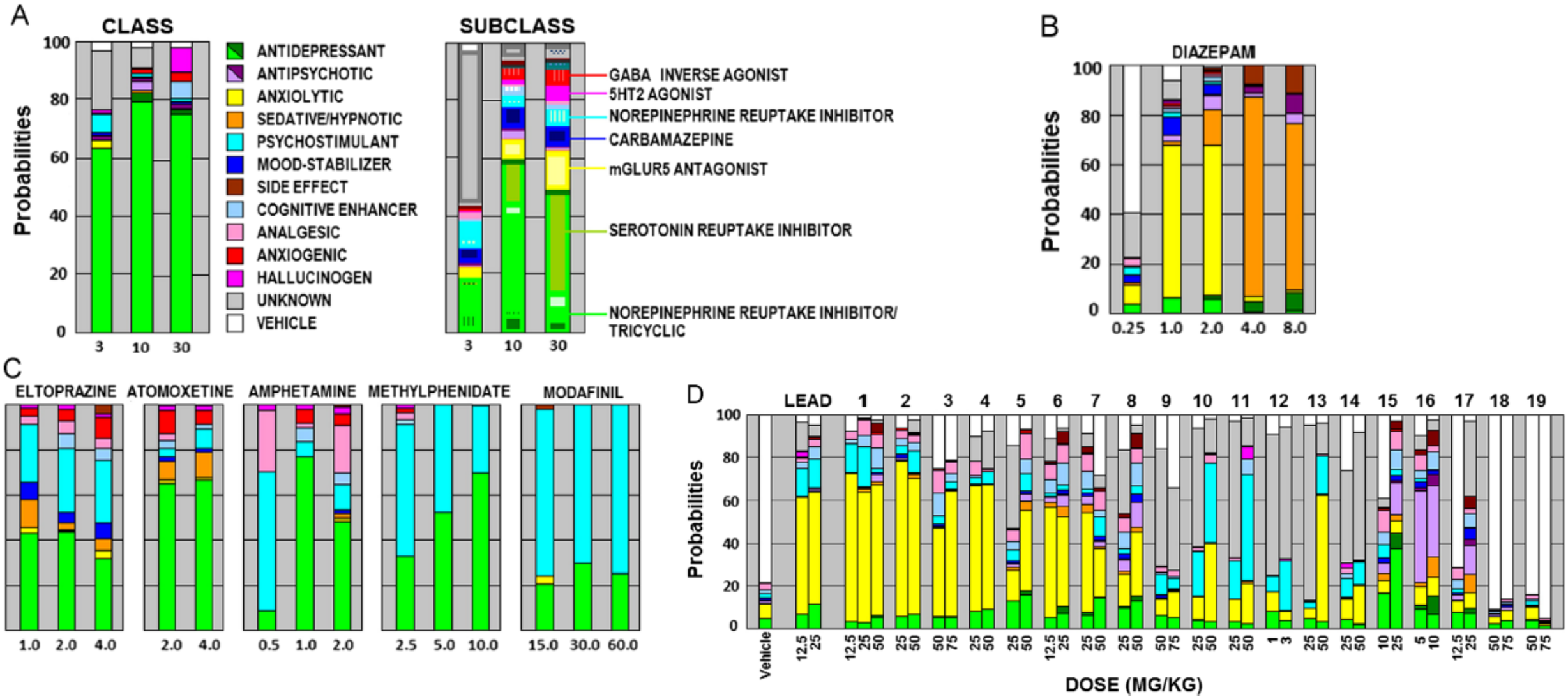

Behavioral high-throughput system: SmartCube

Figure 3

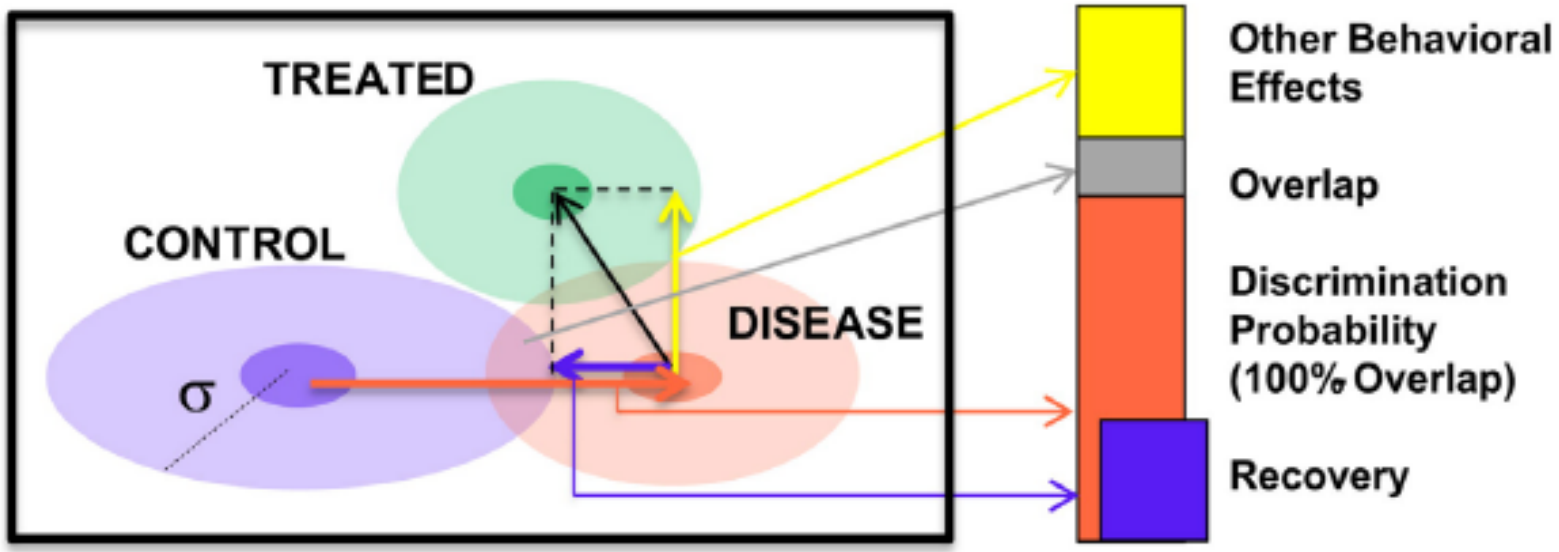

Visualization of a binary discrimination in the ranked de-correlated feature space.

The “recovery signature” graph

Behavioral high-throughput system: SmartCube

Figure 4

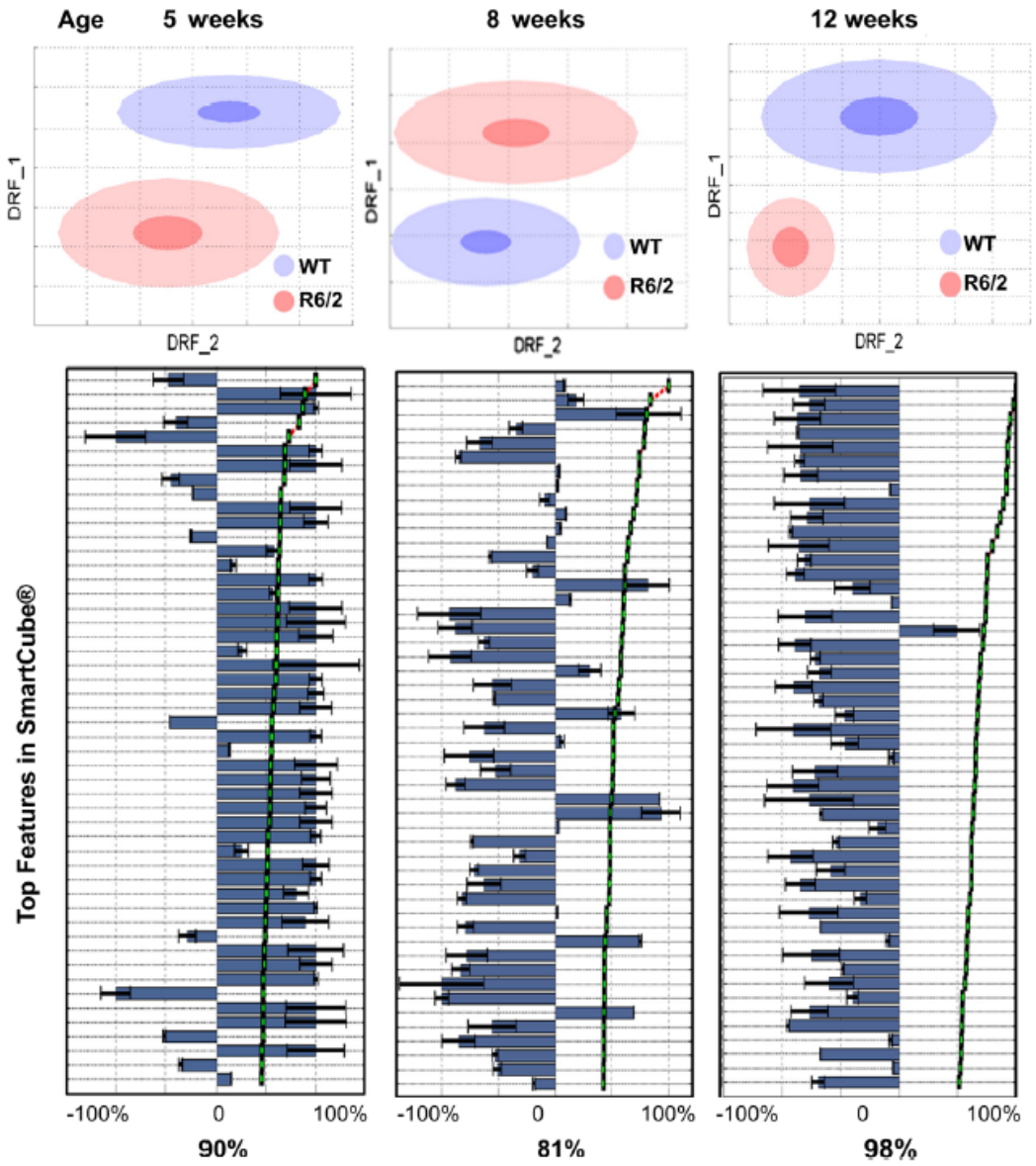

Age specific disease signature of the R6/2 mouse model.

Ranking algorithm:
Difference in feature values and feature ranks (red curve with green squares).

Behavioral high-throughput system: NeuroCube

- Subjects are allowed to freely walk for 5 min in the NeuroCubes system. Digital video acquisition and processing through computer segmentation algorithms.
  - fitted parameters analyzed to extract clips of locomotor behavior.
  - extracts information about gait geometry (stride length, step length and base width) and gait dynamics (stride duration, step duration and swing duration).

- In addition, data acquisition of:
  - Average Speed of the animal.
  - Paw Image intensity, paw contact area, perimeter of contact zone, and paw diameter.
  - Paw Position relative to the center of the body is registered.
  - Body Position as it pertains to movement of the subject. Rhythmicity and limb coordination

Behavioral high-throughput system: NeuroCube

Figure 5

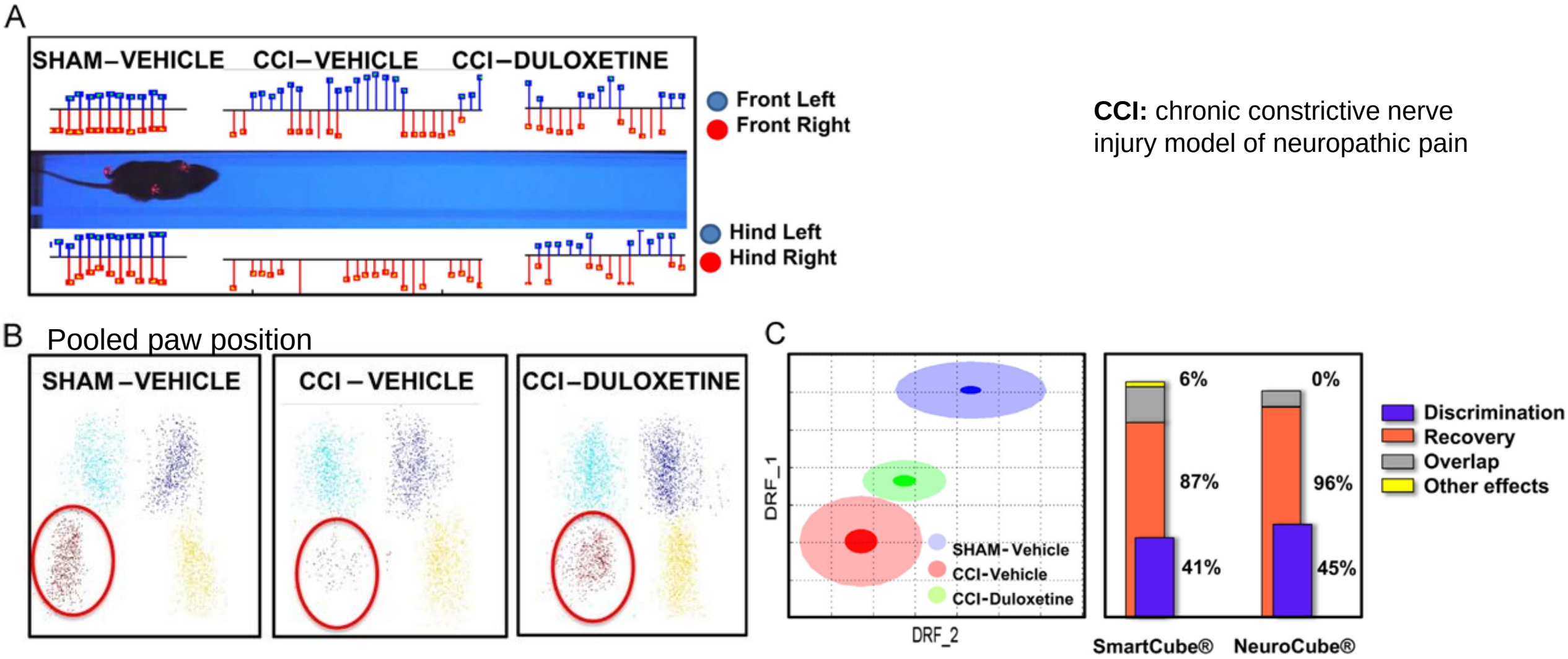

CCI: chronic constrictive nerve injury model of neuropathic pain

Behavioral high-throughput system: PhenoCube

- IntelliCage:

  12/12h light/dark cycle; water available in the corners, food freely available, 8 units for **PhenoCube**, challenging mice with intramaze spatial cues (laminated paper with stripes, two climbung rods, rectangular object in the center)

  16-h water deprivation (home cage) → 72-test session: placement in IntelliCage

  → **Habituation**: water freely available in the corners for 6h

  measures corner visit, nose-poking frequency, alternations)

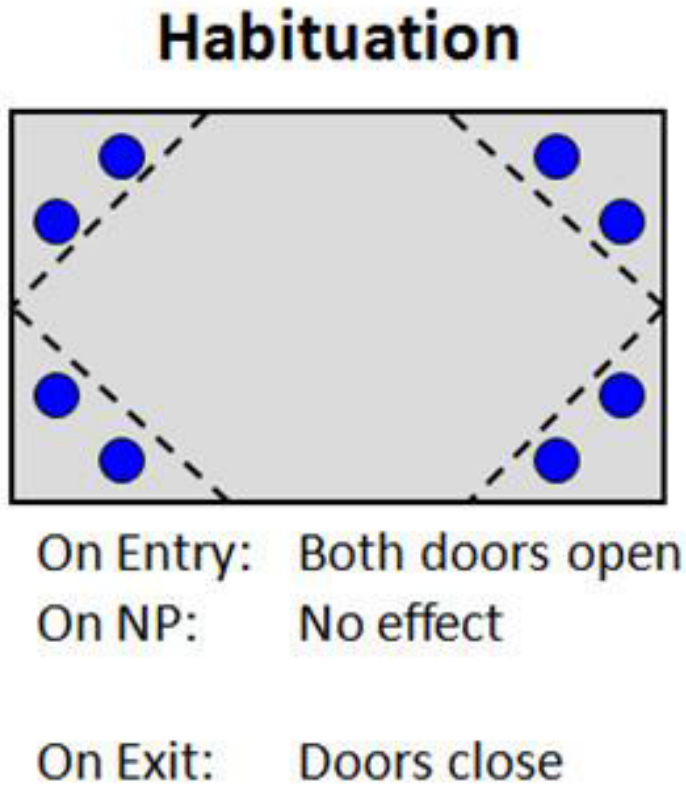

Behavioral high-throughput system: PhenoCube

Alternation: two adjacent active corners for each subject, train animals to switch between, alternate 1, 2, 1, 2, …(calculated within an interval of leaving an active corner and visit a correct corner in 113s or less), nose-poking: only left-hand side provided reward (8s access to water) in active corner 1, right-hand side in 2 (measures frequency of alternation, nose pokes to the correct side, % of correct initial nose pokes in each visit)

Computer vision data: distance traveled, time in locomotion, immobility time, climbing time, rearing, huddling, occlusion (two or more mice togethet)

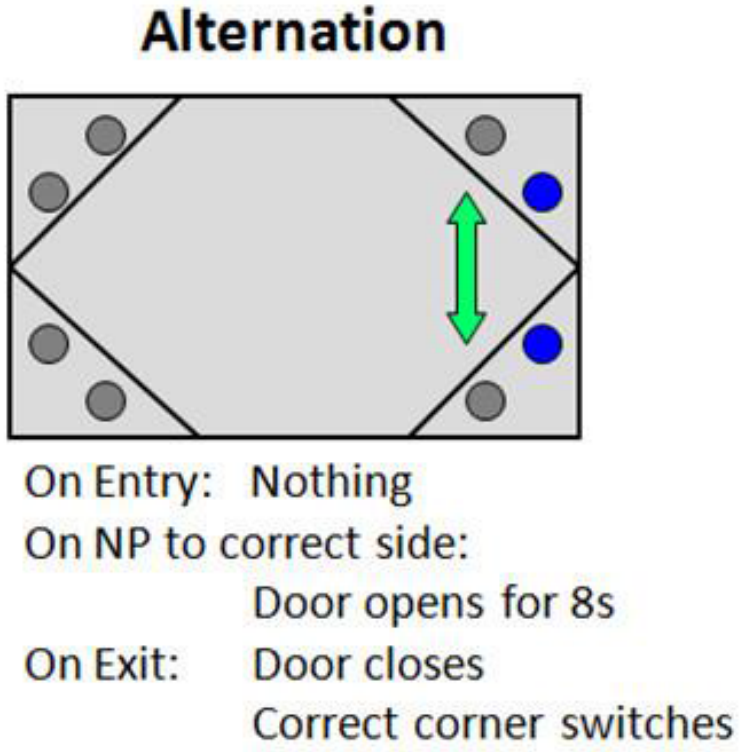

Behavioral high-throughput system: PhenoCube

Figure 6

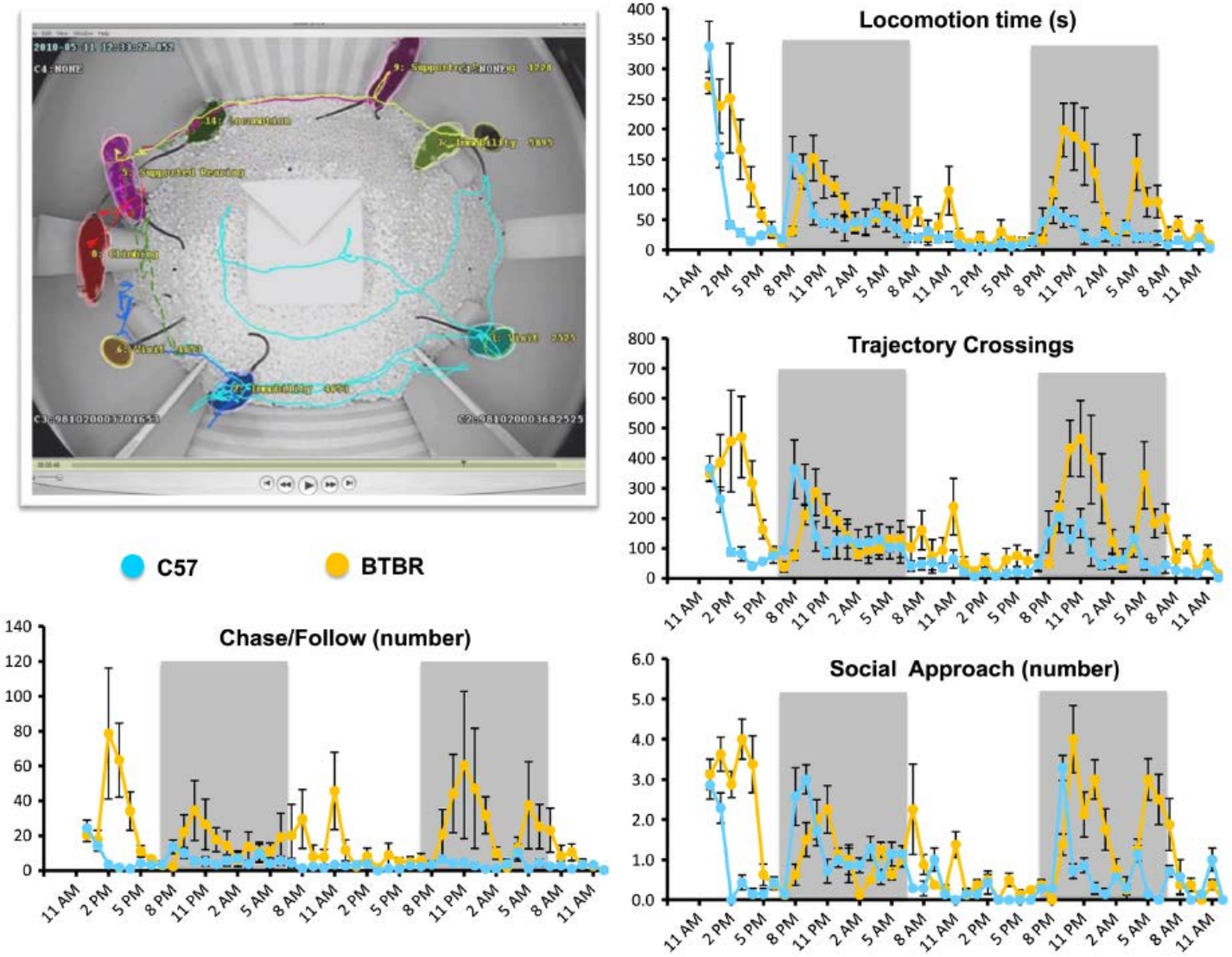

nature COMMUNICATIONS

ARTICLE

Received 15 Jan 2016 | Accepted 27 Apr 2016 | Published 7 Jun 2016

DOI: 10.1038/ncomms11758 OPEN

Human glia can both induce and rescue aspects of disease phenotype in Huntington disease

Abdellatif Benraiss[1], Su Wang[1], Stephanie Herrlinger[1], Xiaojie Li[1], Devin Chandler-Militello[1], Joseph Mauceri[1], Hayley B. Burm[1], Michael Toner[1], Mikhail Osipovitch[2], Qiwu Jim Xu[1], Fengfei Ding[1], Fushun Wang[1], Ning Kang[1], Jian Kang[3], Paul C. Curtin[4], Daniela Brunner[4], Martha S. Windrem[1], Ignacio Munoz-Sanjuan[5], Maiken Nedergaard[1,2] & Steven A. Goldman[1,2,6]

Figure 1

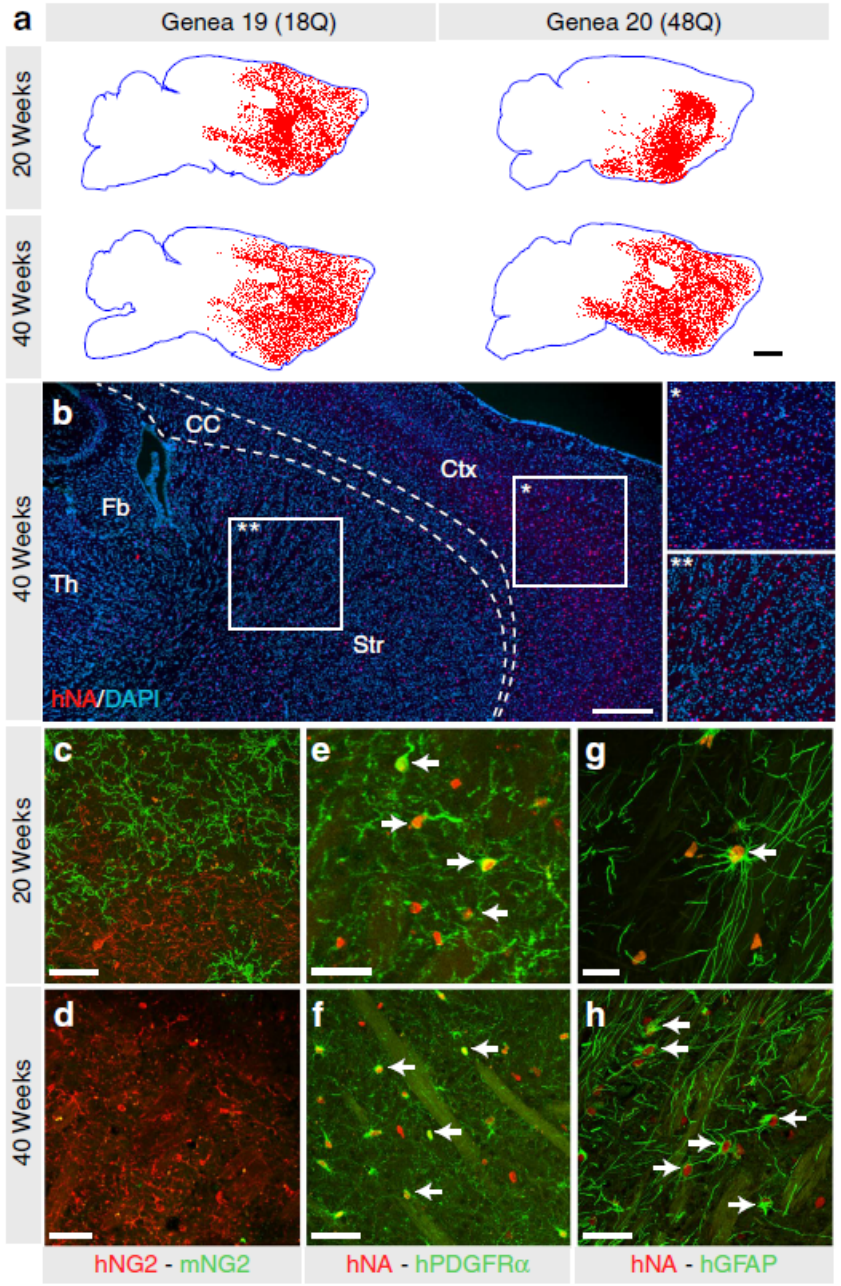

Table 1 | Engraftment of hESC-derived GPCs in normal Htt immunodeficients.

Cell type	Sacrifice	% GFAP$^+$	% Olig2$^+$	Total donor cells	humanNA$^+$/mm^3 striatum
GENEA19 (18Q)	20 weeks ($n=3$)	2.1 ± 0.6	71.8 ± 19.4	74,173 ± 14,305	21,000 ± 3,608
	40 weeks ($n=4$)	1.7 ± 0.5	82.5 ± 8.6	42,807 ± 6,991	9,335 ± 1,341
GENEA20 (48Q)	20 weeks ($n=3$)	2.3 ± 0.4	56.4 ± 7.5	42,520 ± 8,792	10,843 ± 3,323
	40 weeks ($n=4$)	2.2 ± 0.7	72.7 ± 6.3	80,798 ± 7,131	16,126 ± 380

hNA, human nuclear antigen.
Data presented as means ± s.e.m.'s.

Figure 2

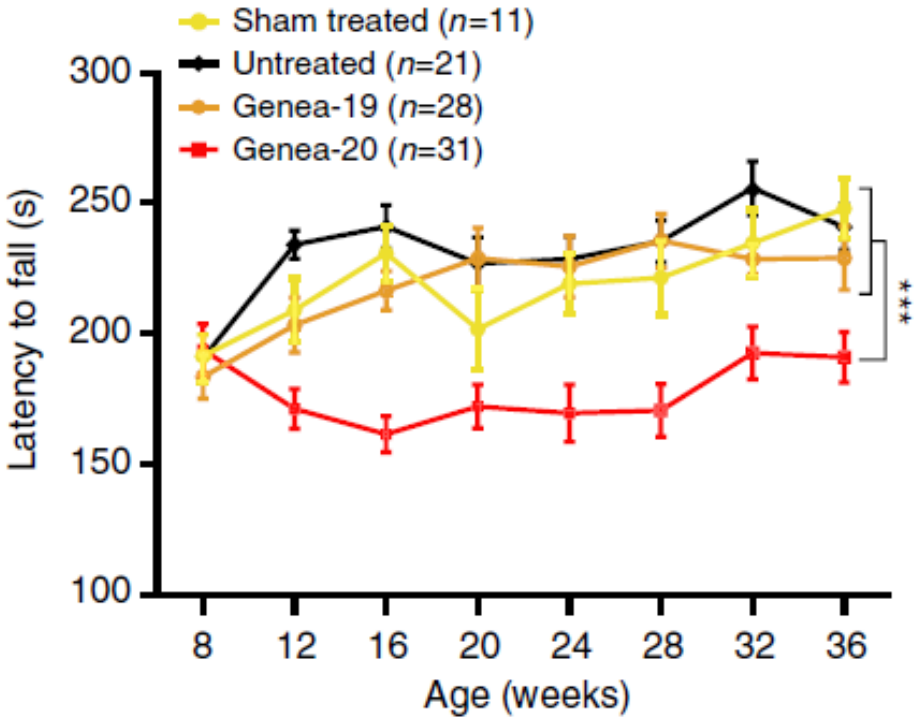

Figure 3

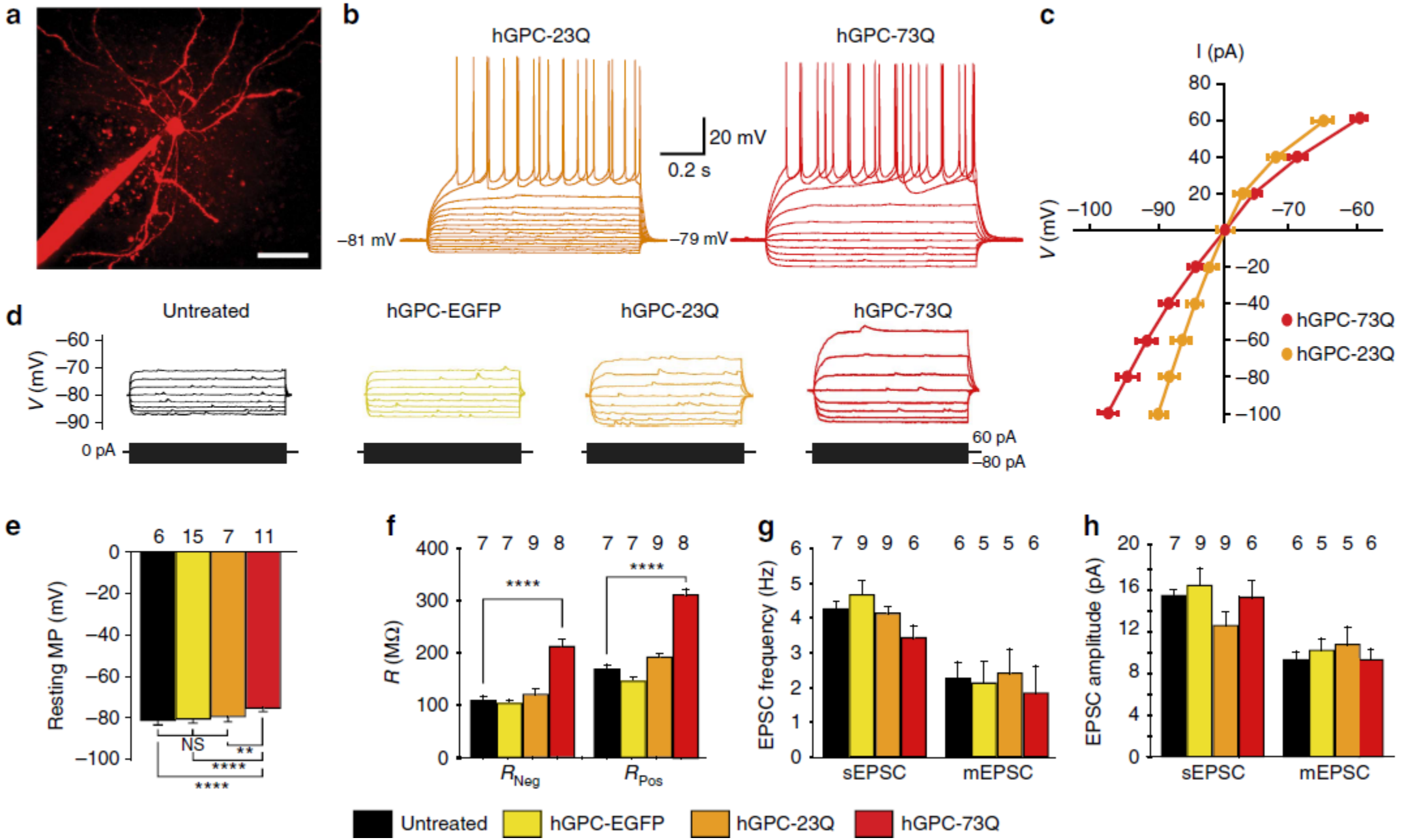
a
b
hGPC-23Q
hGPC-73Q
20 mV
0.2 s
–81 mV
–79 mV
c
I (pA)
V (mV)
hGPC-73Q
hGPC-23Q
d
Untreated
hGPC-EGFP
hGPC-23Q
hGPC-73Q
V (mV)
0 pA
60 pA
–80 pA
e
Resting MP (mV)
6 15 7 11
NS
**
****
****
f
R (MΩ)
7 7 9 8 7 7 9 8
****
****
R_{Neg}
R_{Pos}
g
EPSC frequency (Hz)
7 9 9 6 6 5 5 6
sEPSC
mEPSC
h
EPSC amplitude (pA)
7 9 9 6 6 5 5 6
sEPSC
mEPSC
Untreated
hGPC-EGFP
hGPC-23Q
hGPC-73Q

Figure 4

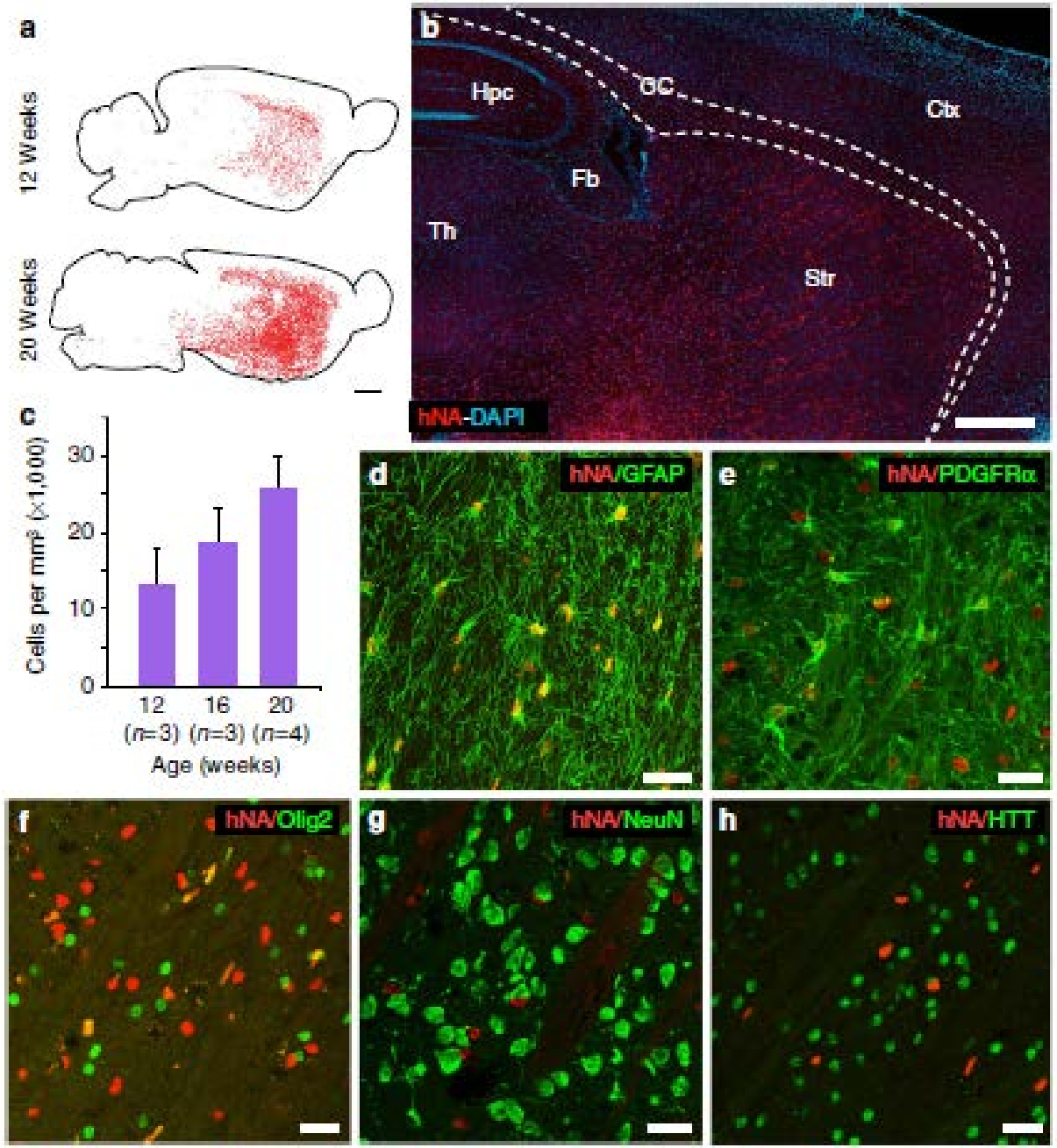

Table 2 | Engraftment of CD44$^+$ GPCs in R6/2 x rag1$^{-/-}$ mice.

Survival time	% GFAP$^+$	% Olig2$^+$	Total cells	hNA$^+$ per mm^3 striatum
20 weeks ($n=4$)	1.7 ± 0.3	45.2 ± 7.8	77,756 ± 21,000	16,651 ± 3,694

hNA, human nuclear antigen.
Data presented as means ± s.e.m.'s.

CD44-sorted hGPCs colonized and replaced endogenous glia within the R6/2rag1/ striatum

Figure 5

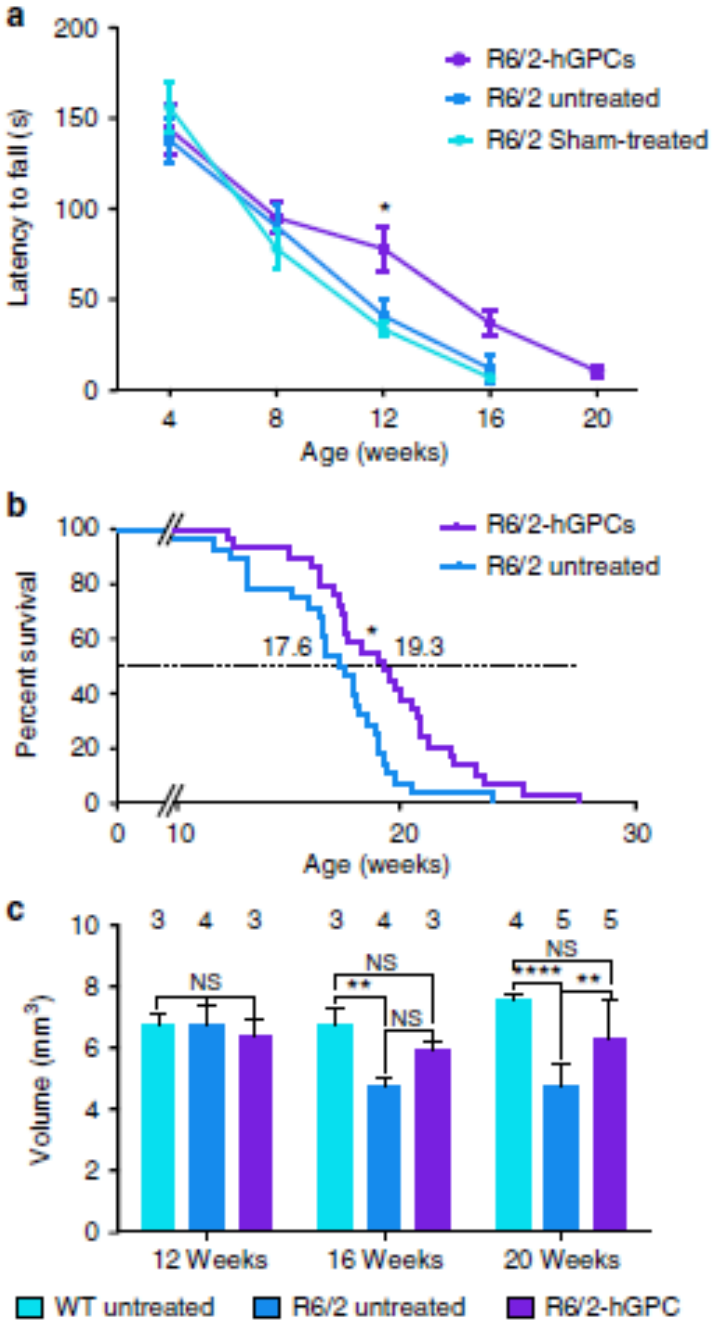

Figure 6

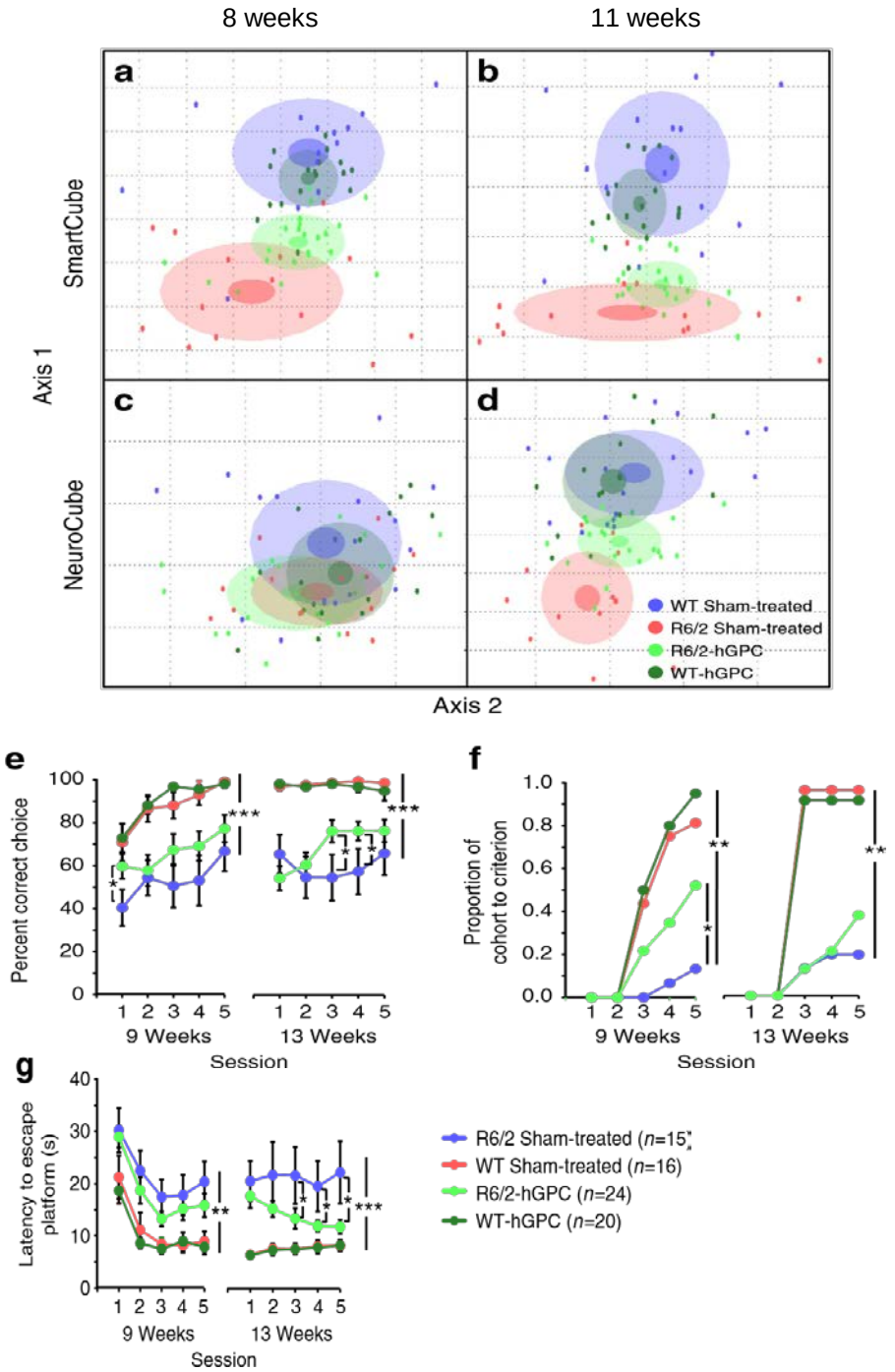

Suppl. Figure 4 SmartCube

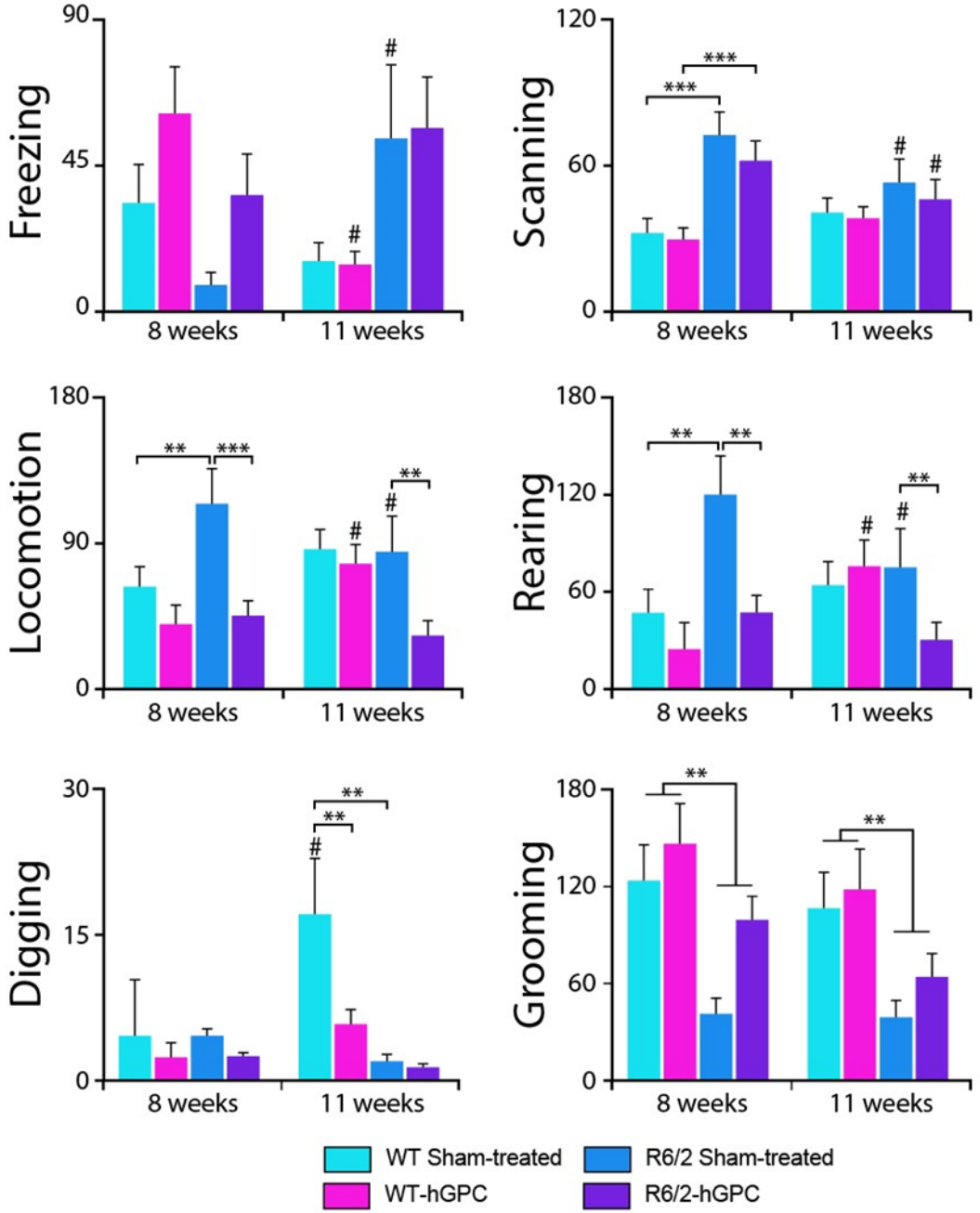

Suppl. Figure 5 NeuroCube

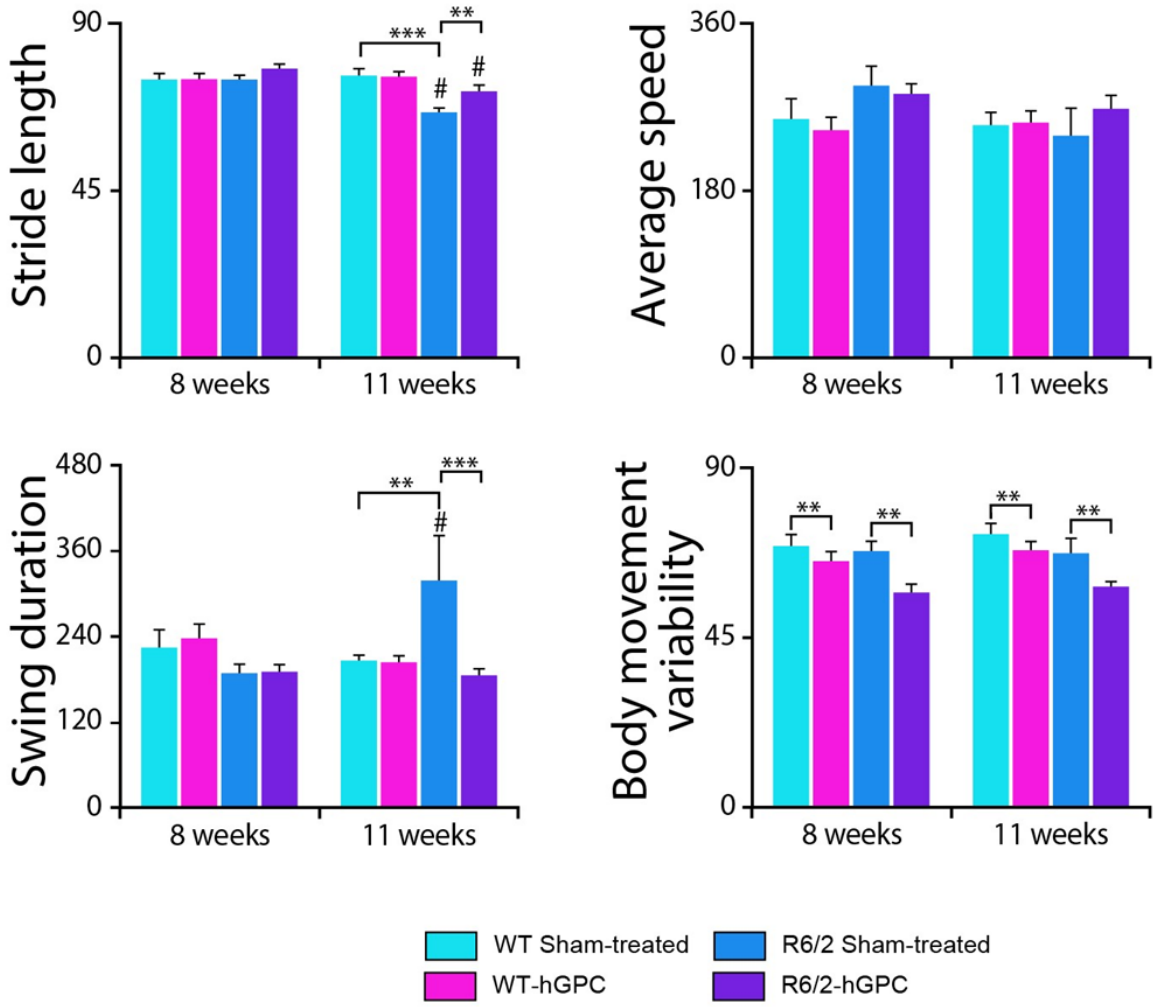

Figure 7

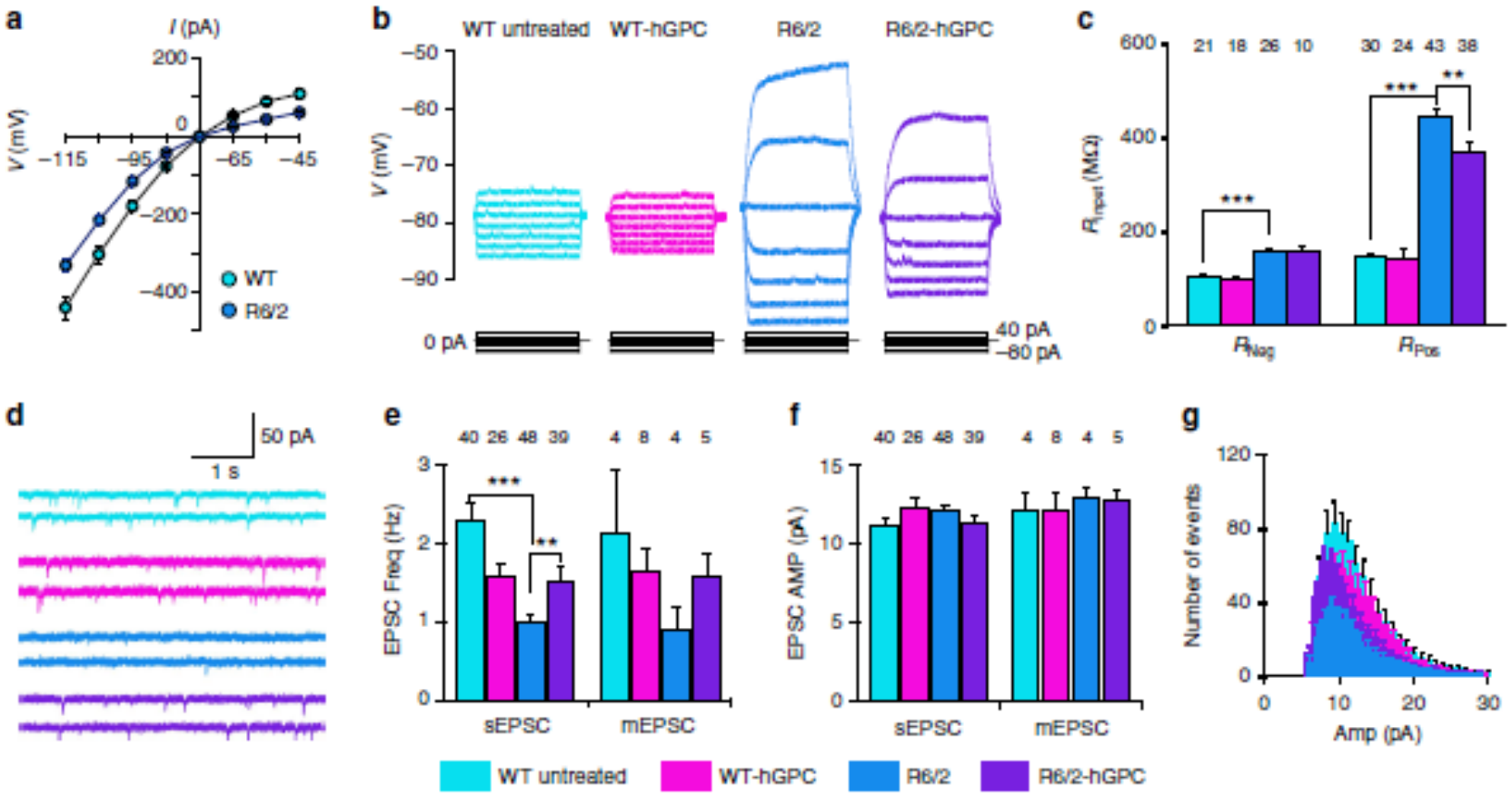

Figure 8

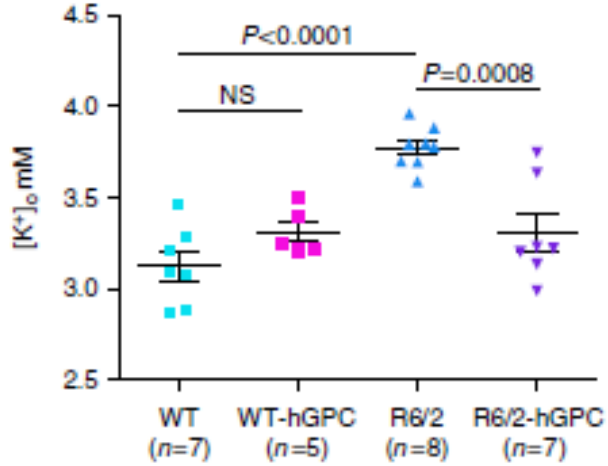

nature biotechnology

Large-scale phenome analysis defines a behavioral signature for Huntington's disease genotype in mice

Vadim Alexandrov[1,4], Dani Brunner[1,4], Liliana B Menalled[1,4], Andrea Kudwa[1], Judy Watson-Johnson[1], Matthew Mazzella[1], Ian Russell[1], Melinda C Ruiz[1], Justin Torello[1], Emily Sabath[1], Ana Sanchez[1], Miguel Gomez[1], Igor Filipov[1], Kimberly Cox[1], Mei Kwan[1], Afshin Ghavami[1], Sylvie Ramboz[1], Brenda Lager[2], Vanessa C Wheeler[3], Jeff Aaronson[2], Jim Rosinski[2], James F Gusella[3], Marcy E MacDonald[3], David Howland[2] & Seung Kwak[2]

Received 11 March 2015; accepted 28 April 2016; published online 4 July 2016; doi:10.1038/nbt.3587

Animals

- Subjects:
  HET mutant mice from six KI lines
  corresponding WT littermates

- Subject selection
  on the basis of of CAG repeats (allows Gaussian distribution)

- Starting point
  16 animals/genotype/sex/line

- Husbandry:
  8-10 animals in experimental cages (rat Opticage); half HET, half WT, same sex
  Removal of extra animals to create final experimental cage (4/4)
  Multi-class analysis: mice with complete dataset (20-30% mice excluded)

	CAG repeat mean	Standard deviation	Min CAG repeat	Max CAG repeat
HdhQ20	20.01	0.25	18	21
HdhQ50	50.34	0.58	49	52
HdhQ50neo	50.19	0.36	49	51
HdhQ80	87.08	2.26	80	92
HdhQ92	102.60	2.13	98	110
HdhQ111	125.35	3.90	110	134
CAG 140	147.58	6.18	136	181
zQ175	204.08	5.02	189	215

Figure 1

Discrimination between wild-type and HET mice.

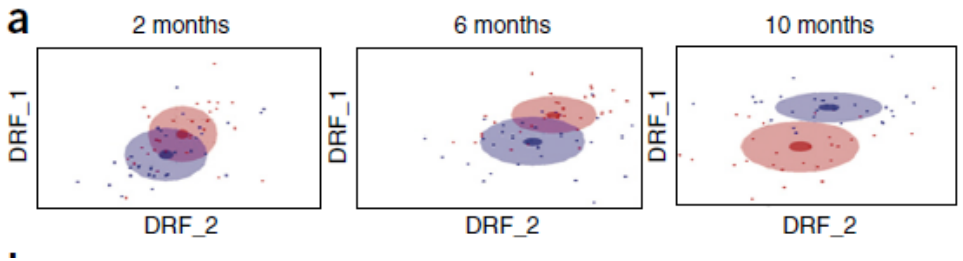

HET mice from the zQ175 line (blue) compared to wild-type littermate controls (red).

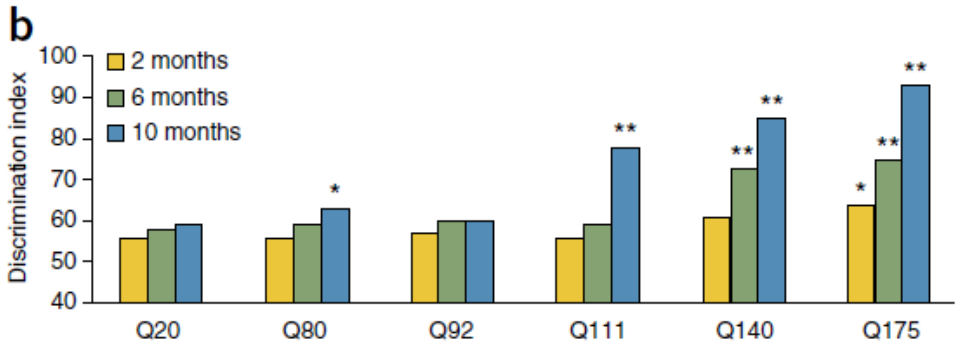

Discrimination values for all CAG models against the corresponding WT controls

Figure 2

Performance of the CAG model during training and testing as assessed by regression on predicted versus observed CAG-repeat length.

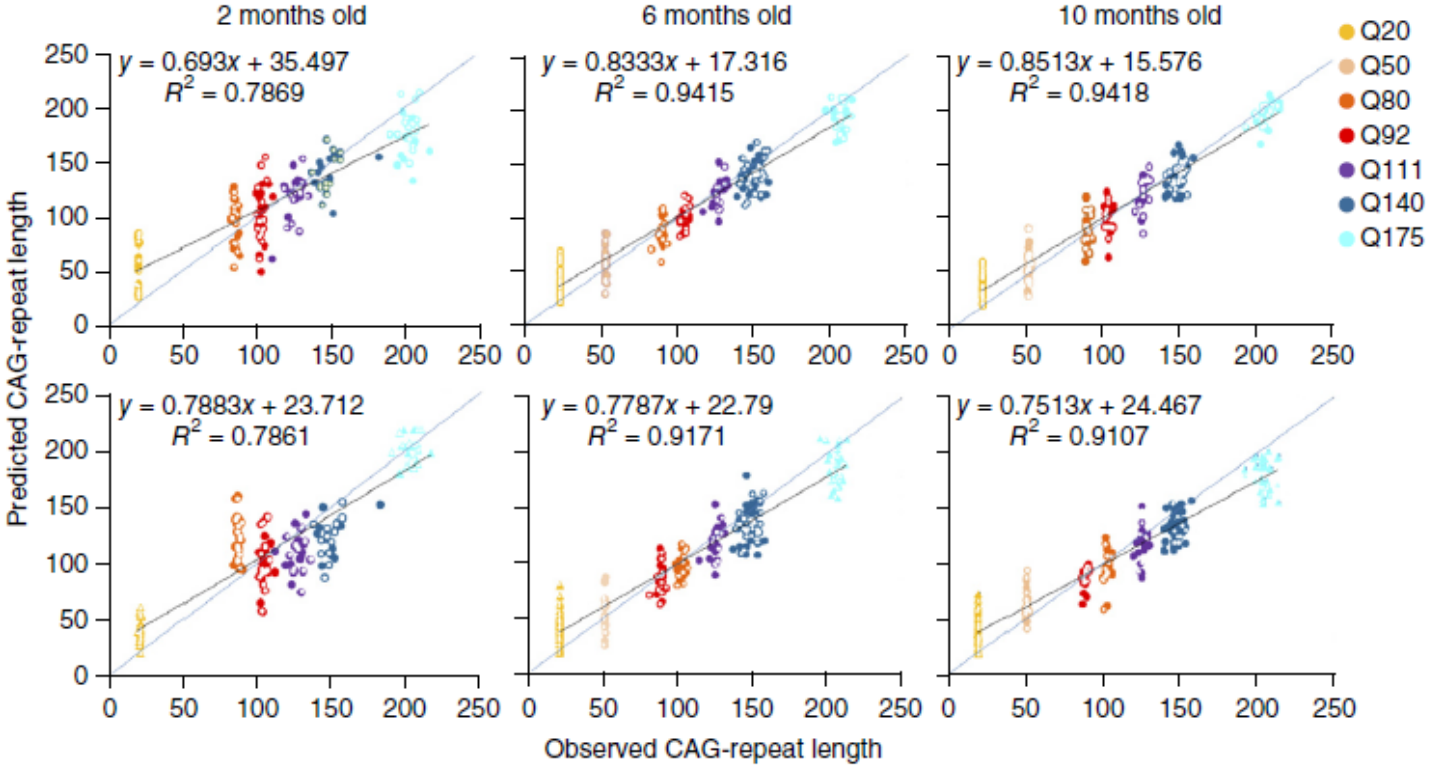

Top: the performance of the CAG models during prediction of CAG-repeat length for one example (LOOCV) not included in the training set

Bottom: to challenge the combined-sex model in a more stringent manner, we left out a whole line and trained with the remaining lines

regression lines black
identity lines blue)

Figure 3

Prediction of the ‘blinded line’ by the SVR CAG model (10-month-old mice).

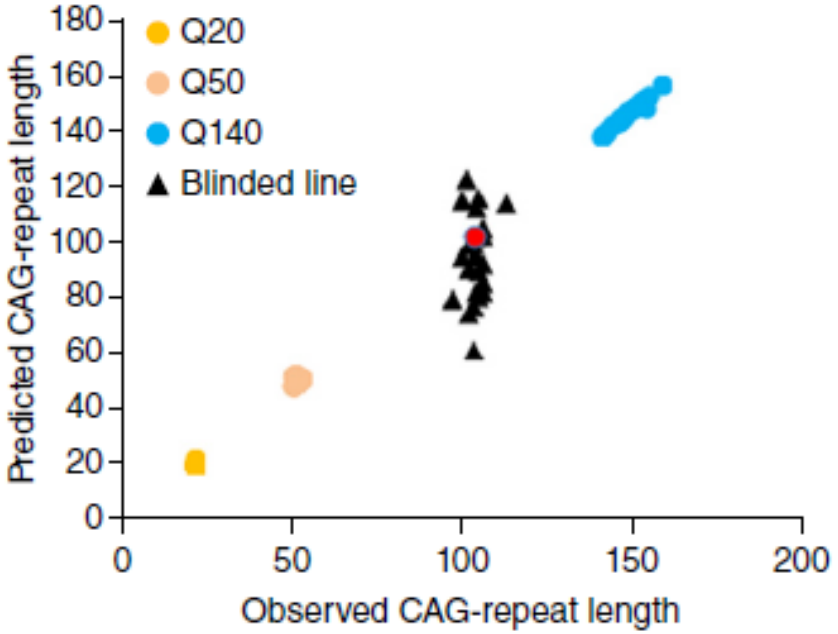

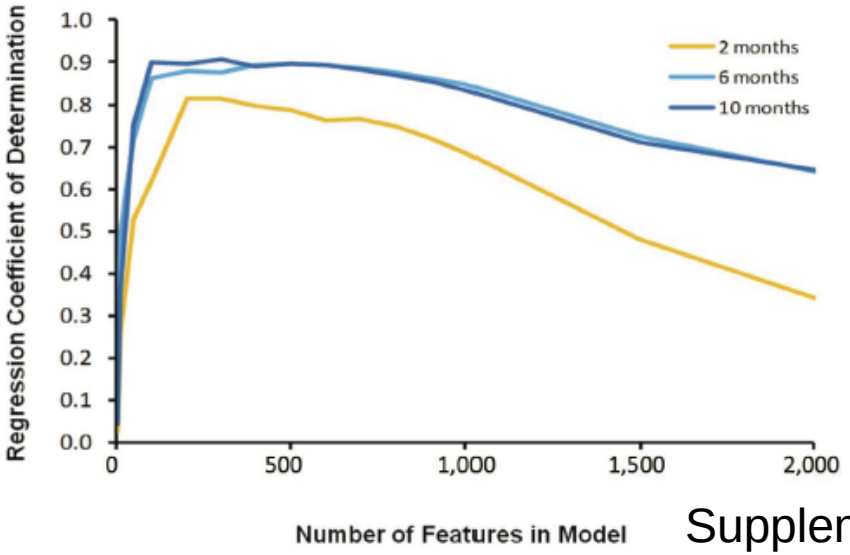

Figure 4

Projection of all Q lines onto the decorrelated ranked feature (DRF) plane defined by Q20 and Q175 lines at 6 months of age.

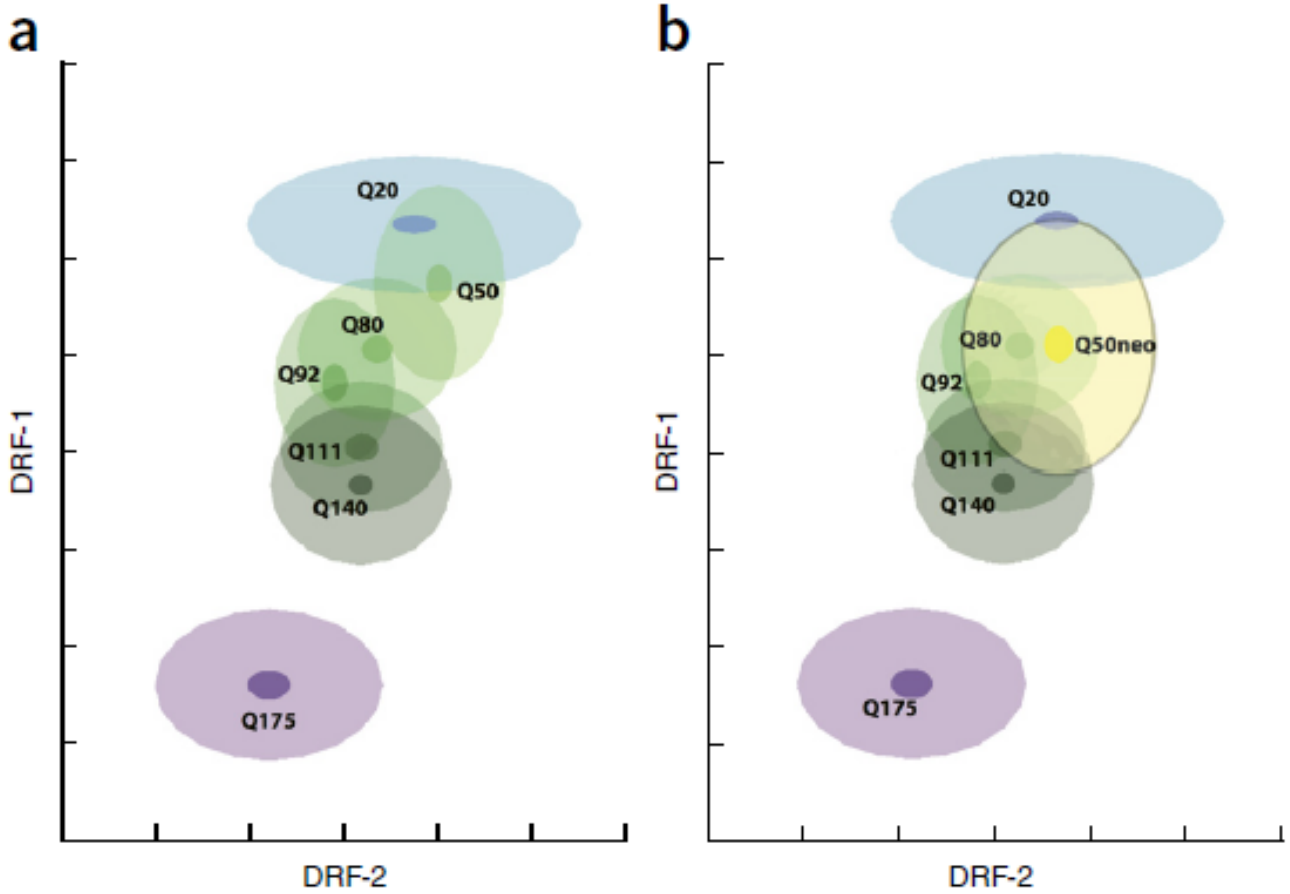

Supplementary Figure 3

Figure 5

Top-feature score changes across different CAG-repeat lengths and ages.

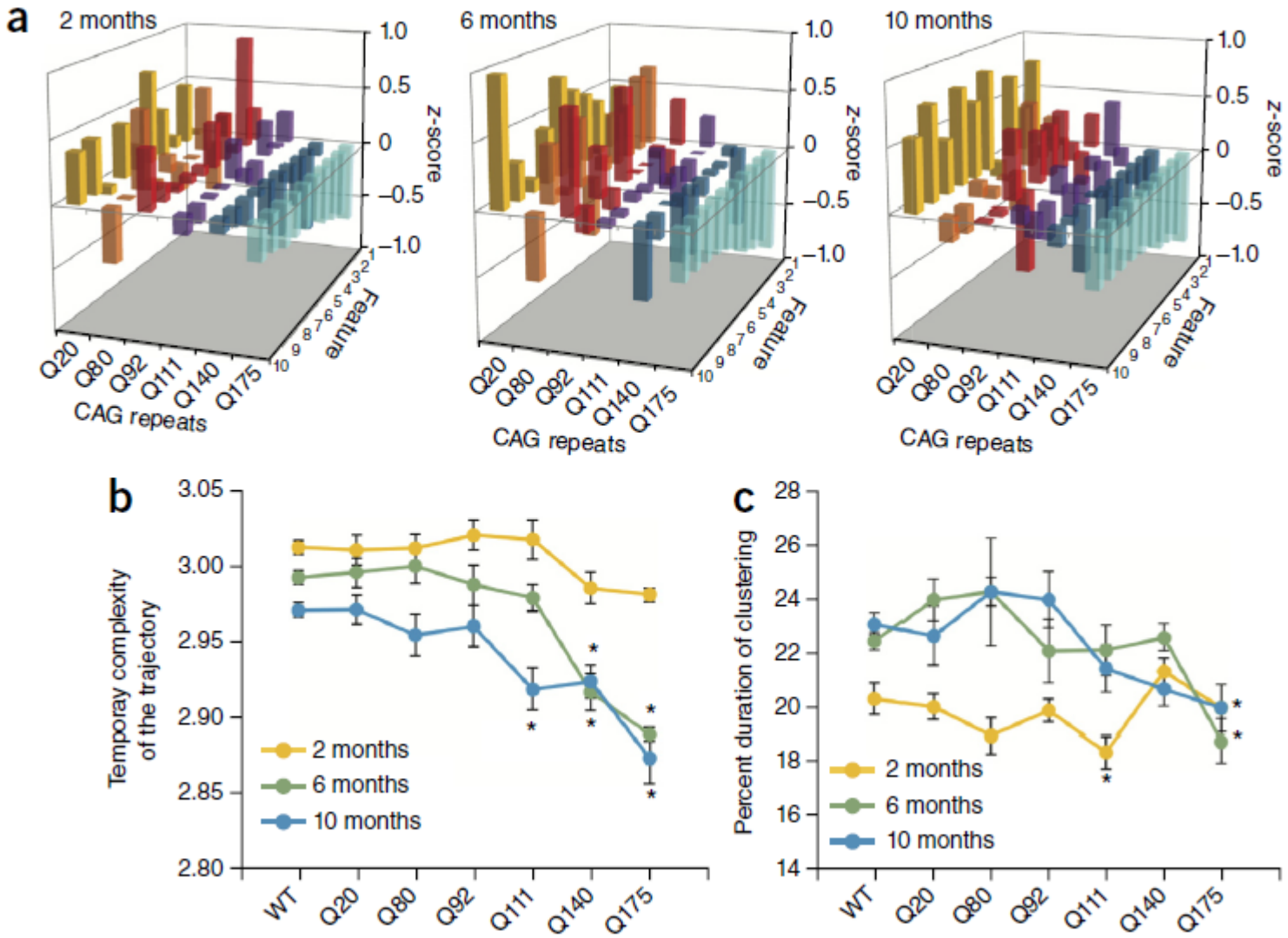

Figure 6

LOOCV performance of the age model during training and testing as assessed by regression on the predicted versus observed age.

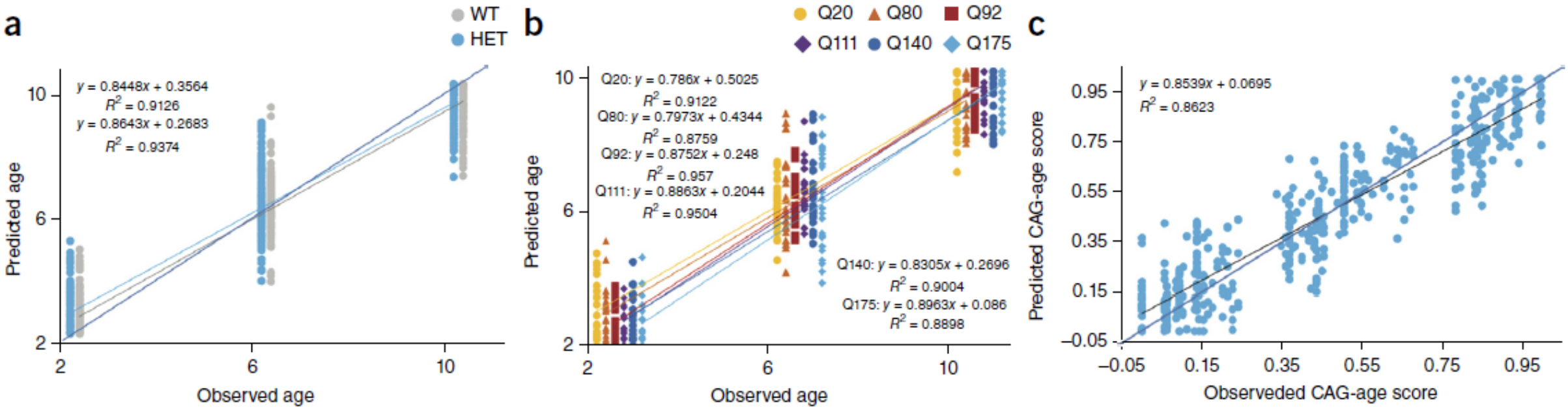

Summary

- Tasks which tackle higher cognitive function have to be performed separately.
- Signatures for specific drugs as well as for disease models could be assessed in an animal-friendly high-throughput manner
- Signatures give rise even to subtle changes in behavior
- Signatures indicate rescue of disease features and/or potential treatment
- Selected behavioral signatures for age and CAG-repeat length could robustly distinguished between mouse lines
- The correct repeat length of a blinded mouse line could be predicted
- Sufficient discriminatory power to accurately predict genotype required combined analysis of >200 phenotypic features.
- Results suggest that autosomal dominant disease-causing mutations could be predicted through the use of subtle behavioral signatures that emerge in large-scale, combinatorial analyses.
- Provides an open data platform that could be shared with the research community to aid efforts focused on understanding the pathways that link behavioral consequences to genetic variation in Huntington’s disease.